

# DynMat, a network that can learn after learning

Jung Hoon Lee<sup>1</sup>

<sup>1</sup>Allen Institute for Brain Science, Seattle WA

## Abstract

To survive in the dynamically-evolving world, we accumulate knowledge and improve our skills based on experience. In the process, gaining new knowledge does not disrupt our vigilance to external stimuli. In other words, our learning process is ‘accumulative’ and ‘online’ without interruption. However, despite the recent success, artificial neural networks (ANNs) must be trained offline, and they suffer catastrophic interference between old and new learning, indicating that ANNs’ conventional learning algorithms may not be suitable for building intelligent agents comparable to our brain. In this study, we propose a novel neural network architecture (DynMat) consisting of dual learning systems, inspired by the complementary learning system (CLS) theory suggesting that the brain relies on short- and long-term learning systems to learn continuously. Our experiments show that 1) DynMat can learn a new class without catastrophic interference and 2) it does not strictly require offline training.

## Introduction

Our knowledge expands gradually by gaining new knowledge, and our skills improve based on experience. The exact underlying mechanisms of this ‘continuous’ learning remain elusive, but human learning has two distinct properties. First, our learning process is accumulative. If we “unlearn” previously obtained knowledge to accept new knowledge/skills, our brain would remain static, and our intelligence would not improve. Second, learning new skills/knowledge does not negate our response to external stimuli. We can concentrate on reading or studying but still hear fire alarms. This ‘online’ learning prepares us for unexpected events. However, building an artificial learning system with accumulative and online learning abilities poses immense challenges. ANNs (Artificial Neural Networks) including deep neural networks (DNN) are trained during an offline training period, in which all necessary examples need to be available, and they suffer catastrophic interference; that is, “old learning” is disrupted by “new learning”; see (Ratcliff, 1990) for details. In this study, learning without catastrophic interference or offline training is referred to as ‘continuous learning’.

Then, how does the brain learn continuously? The complementary learning system (CLS) theory proposes that the brain utilizes short- and long-term learning systems for continuous (or continual) learning (Norman and O'Reilly, 2003; O'Reilly et al., 2014). The short-term learning

system relies on fast memory system to store new experience (or examples) using sparse and non-overlapping codes (representations); see also (Parisi et al., 2018). Due to its sparse representations, the interference between old and new items (i.e., knowledge) are minimized. The information stored in the short-term learning system can be replayed into a more effective learning system which utilizes dense and overlapping codes for information storage. Consistent with the CLS theory's emphasis on memory, memory-augmented networks have been proposed to improve learning ability of neural networks (Graves et al., 2014; Santoro et al., 2016). For instance, incorporating memory into networks was proposed for implementing one-shot learning (Santoro et al., 2016) and alleviating catastrophic interference (Lüders et al., 2017; Parisi et al., 2018). In these earlier studies, examples (i.e., sensory inputs) are stored in external memory units (Graves et al., 2014; Santoro et al., 2016) or neurons (computing nodes in the networks) (Hochreiter and Urgen Schmidhuber, 1997; Parisi et al., 2018). Interestingly, theoretical studies in neuroscience suggested that the brain can utilize synapses to store information (Choi et al., 2018; Kleim et al., 2002; Mayford et al., 2012; Mongillo et al., 2008). For instance, Diehl and Cook (Diehl and Cook, 2015) suggested that the brain's spike-time dependent plasticity, which is thought to underlie learning capability of the brain, can imprint inputs (examples) to synapses.

Inspired by these studies, we hypothesized that synapses can underlie short-term learning system in the CLS theory, which allows networks to learn continuously (without offline learning or catastrophic interference). To address this hypothesis, we constructed the 'dynamic matching machine' (DynMat), in which synapses store examples and partake in the short-term learning system. DynMat learns a new example quickly by imprinting it to a set of weights converging to a neuron. With the new example imprinted on synapses, the short-term learning system in DynMat calculates similarities between the present example and previously stored examples and utilize them to predict the class (i.e., label) of untrained examples. Also, DynMat has a long-term learning system, as proposed in CLS theory, which can be trained offline.

In our study, we tested whether DynMat can learn continuously (without offline training or catastrophic interference), as it learns examples of a new class after learning examples of two classes. Our experiments show that DynMat's short-term learning system learns new examples from the third-class (a new class) with minimal interference (from other two classes that were previously trained); in fact, it recognizes untrained examples from the third-class, although it has not been trained offline. Additionally, the long-term learning system can be trained offline to improve DynMat's performance on test examples of all three classes. These results support that synapses could effectively and efficiently implement the short-term learning system of the CLS theory. Therefore, DynMat is a simple but effective realization of the CLS theory.

## Results

The schematics of DynMat are illustrated in Fig. 1A; it consists of matching layer (ML), short-term learning module (STLM) and long-term learning module (LTLM), which is consistent with the CLS theory. ML, the first stage of DynMat, receives external inputs and forwards outputs to STLM and LTLM. The external inputs  $\vec{x^k}$  to ML are normalized to have unit lengths (Eq.1), and ML stores these normalized examples by imprinting them to synaptic connections. As a result, a synaptic input  $h_i$  to a ML neuron  $m_i$  is proportional to cosine similarities between a present

example and examples previously stored in synapses targeting the neuron  $m_i$  (Eq. 1). The number of stored examples is not fixed. Instead, it grows when a present input is substantially different from the previously introduced examples; specifically, a new ML neuron is added if no input  $h_i$  is higher than the threshold value  $\theta$ . This comparison is conducted with examples within the same class. For instance, an instantiation of digit 2 is compared to other digit 2 instantiations stored in ML.

STLM is a linear layer working as a temporary learning system, in which each neuron represents (codes) a class (Fig. 1A); in this study, there are maximally 3 neurons in STLM because examples are drawn from three classes only. STLM does not need to be trained offline to classify inputs from ML neurons. Instead, each ML neuron is exclusively connected to a STLM neuron according to its class (Eq. 2). For instance, when an instantiation of digit ‘2’ is imprinted to synaptic weights converging to a newly inserted ML neuron, the new ML neuron is connected to the STLM neuron representing the class (i.e., digit) ‘2’. Specifically, inputs to STML neurons are nonlinear summations of ML outputs (Eq. 2).

LTLM corresponds to the CLS theory’s long-time learning system. Since it is proposed to utilize distributed and overlapping codes, we constructed LTLM using a hidden-layer perceptron known to use overlapping representation (Hertz et al., 1991). In principle, there is no restriction on the structure of LTLM. Any network that can be trained offline to perform tasks effectively (e.g., classification in this study) can be used as a LTLM. We selected a hidden-layer perceptron due to its well-documented learning power (Hertz et al., 1991; LeCun et al., 1998). As seen in Eq. 3, inputs to LTLM are the linear summations of inputs of ML neurons; that is, the gain of ML neurons for LTLM is set to 1. With ML outputs, LTLM is trained using a common backpropagation with mean-squared estimated error (see Methods).

In this study, we tested if DynMat can learn continuously using three datasets (MNIST, fashion-MNIST and CIFAR-100) (Krizhevsky, 2009; LeCun et al., 1998; Xiao et al., 2017); see Methods. The goal is to test whether DynMat can learn without catastrophic interference or offline training, not to compare DynMat’s performance to other learning algorithms and networks. Regardless of datasets, we used the same protocol as follows:

1. We used all training examples of the first two classes to build ML and STLM. Then, LTLM was trained with linear outputs of ML (Eq. 3).
2. We exposed DynMat to examples of the third-class and constructed ML and STLM accordingly. Whenever a new ML neuron was added to ML, the error rates of STLM on test examples of all three classes were estimated.
3. We trained LTLM with training examples of all three classes and tested its performance on the test set.

The first step is designed to generate the initial state of DynMat to test its continuous learning ability. The second step addresses DynMat’s ability to learn without interference between old and new learnings or offline training. The aim of the third step is to compare the classification fidelity between LTLM and STLM.

Since ML is fully connected to the input layer, DynMat can replace any fully connected networks including multi-layer perceptrons (MLPs), which have been trained to perform numerous tasks (Hertz et al., 1991). For instance, MLPs can learn to read out handwritten digits by looking at 28-by-28 gray pixel images (LeCun et al., 1998). Recently, however, the fully

connected layer network is used as a final classifier in DNNs. That is, a fully-connected layer can work as a standalone (e.g., MLPs) learning system or as an embedded (e.g., the final classifier in DNNs) one. Below, we describe the experiments, in which DynMat is tested as both a standalone system (Fig. 1A) and an embedded one (Fig. 1B).

### DynMat as a standalone learning system

We asked if DynMat can work as a standalone system similar to MLPs by training it with raw pixel images included in MNIST and fashion-MNIST.

For MNIST dataset, we used training and test examples of three digits (i.e., classes) ‘0’, ‘1’ and ‘2’. As stated above, we first constructed ML using all examples of ‘0’ and ‘1’ in the training set and connected ML to STLM neurons, using one-to-one exclusive connections (Eq. 2). We varied the threshold value  $\theta$ , which is compared to input  $h_i$  to ML neuron  $m_i$  (see Methods). As the threshold value  $\theta$  increases, the size of ML grows (Fig. 1C). Then, we trained LTLM using the common backpropagation (Methods). After this offline-training, LTLM reliably recognizes the examples in the test set (Fig 1C) over a wide range of threshold values; the classification error is extremely low because LTLM is trained with the two classes of digits (0 and 1) only.

Next, we introduced digit ‘2’ training examples (the third-class examples) to DynMat. When presenting each example of digit 2, the inputs to ML neurons that store examples of ‘2’ are compared with the threshold value  $\theta$  to determine whether the current example is substantially distinct from the earlier examples and needs to be stored. When a new neuron is added to ML to store a new example, it is connected to the neuron representing digit ‘2’ in STLM; all new examples are drawn from digit 2 training examples. Whenever a new ML neuron was added, we evaluated STLM’s classification error on all test examples of three digits (‘0’, ‘1’ and ‘2’). Figure 2A shows the changes in measured error rates with  $\theta=0.5$  during the introduction of the third-class. Figures 2B-D show the same results, but a distinct  $\theta$  is used in each case. As  $\theta$  becomes higher, the performance of STLM is improved. We made two germane observations independent of  $\theta$ . First, as the number of digit ‘2’ examples stored in ML, shown in x-axis, increases, the error rate of STLM on two digits (0 and 1), which was previously trained, rises. Second, the error rate of STLM on the new digit ‘2’ declines.

The increasing error rate on the two digits (0 and 1) can be the result of the interference between old and new learning, but it should be noted that this increasing error rate is quite limited. Importantly, the error rate on digit 2 decreases rapidly. That is, STLM learns digit ‘2’ examples with minimal interference from previous learning of digits 0 and 1. After seeing all available examples of digit 2, STLM recognizes all three examples at a low error rate ( $\sim 0.1\%$  with  $\theta=0.8$ , shown in Fig. 2D). As expected, the number of examples of all three digits stored in ML increases, as  $\theta$  increases (Fig. 2E). Finally, we trained LTLM with all three digits and compared the error rates on the test set between LTLM and STLM (Fig. 2F). STLM produces more errors, but the difference between STLM and LTLM becomes smaller, as  $\theta$  increases.

It is rather unexpected that STLM and LTLM showed almost the same level of performance, even though STLM is not trained offline. This may be attributed to the simplicity of MNIST dataset. Thus, to further test DynMat as a standalone learning system, we also trained DynMat with the fashion-MNIST, a proposed drop-in replacement of MNIST (Xiao et al., 2017). Fashion-MNIST includes images of 10 fashion items such as shoes (see Methods). After randomly selecting 3 items out of 10 items in the dataset, we repeated the same experiments

above. Figures 3A-D show the error rate of STLM on test examples with various threshold values during the exposure of the third-class. STLM produces more errors on fashion items (fashion-MNIST) than on handwritten-digits (MNIST), but we observed the same trend. First, the classification error on the third-class object improves rapidly with minimal increase of the error on the test examples of the first two classes (Figs. 3A-D); the  $x$ -axis represents the number of examples of the third-fashion item stored in ML. Second, the difference between STLM and LTLM becomes smaller, as  $\theta$  increases. Finally, we tested DynMat by conducting 10 independent experiments, in which three fashion items were randomly chosen. In all experiments, the ML size increases (Fig. 3E), and STLM's classification fidelity is improved (Fig. 3F), as  $\theta$  increases.

The results above suggest 1) that the combination of ML and STLM allows DynMat to learn a new class after learning other classes without offline training or catastrophic interference and 2) that LTLM can be re-trained with all classes including the new one and provides a better classification fidelity when DynMat can afford offline training.

### DynMat as an embedded learning system

In recent breakthroughs in deep learning (Lecun et al., 2015; Schmidhuber, 2015; Vargas et al., 2017), fully connected networks are embedded into deep neural networks to classify outputs of convolutional networks (ConvNets); the outputs of ConvNets are often referred to as features of visual images from databases. Given the explosive applications of deep neural networks, it is important to test if DynMat can work with the features detected by ConvNets. To this end, we used residual deep neural networks (ResNet) proposed by (He et al., 2015) as feature detectors. Specifically, we replaced the fully connected layer in ResNet with DynMat (Fig. 1B) and tested the classification error of DynMat using the same experimental protocol. In this experiment, we used the 'ResNet20' publicly available (Idelbayev, 2018); ResNet20 will be referred to as RestNet hereafter. It should be noted 1) that the ResNet was trained with CIFAR-10 dataset instead of CIFAR-100 used to test DynMat and 2) that we tested DynMat using the three visual objects (i.e., classes) randomly chosen from CIFAR-100. If feature detectors (i.e., ResNet in this study) are trained with CIFAR-100 dataset, inputs to DynMat (which replaced the fully connected layer in the original ResNet) may be highly optimized for classification, and the performance of DynMat as a continuous learning system can be overestimated. To avoid this potential bias, we used pretrained ResNet with CIFAR-10 dataset.

As with experiments with MNIST and fashion-MNIST, we measured the classification error of STLM on test examples during the exposure of the third-class objects (Figs. 4A-D). The increase of error rate on the two previously trained class objects is much slower than the reduction of error rate on the third-class object, suggesting that STLM learns the features detected by ResNet without offline training and catastrophic interference, as discussed above. We also performed 10 independent experiments, in which 3 visual objects were randomly drawn out of 100 class objects. In all experiments, as  $\theta$  increases, the number of stored examples increases (Fig. 4E), and the classification error of STLM approaches that of LTLM (Fig. 4F), supporting that DynMat can work as an embedded learning system as well as a standalone system.

### DynMat as a self-contained learning system

So far, we have discussed the classification error of LTLM trained with all available training examples to estimate the upper bound of LTLM's classification fidelity. However, as the offline training of LTLM requires an external memory storage of training examples, it could be

expensive for agents to accumulate experience over a long period. As DynMat stores a subset of examples in synapses in ML, the stored examples can be used to train LTLM to remove external memory. Thus, we asked if the examples stored in ML could suffice to train LTLM to perform reliable classification. Since the number of examples in ML depends on  $\theta$ , we measured the classification error of LTLM trained with examples stored in ML with varying  $\theta$ . Specifically, we compared a LTLM trained with CIFAR-100 examples stored in ML against a LTLM trained with a full training set. Additionally, we compared the classification error of LTLM to that of STLM. We note 1) that the precision of LTLM on test examples improves, as  $\theta$  becomes higher (Fig. 5A) and 2) that the classification error of LTLM trained with stored examples in the ML becomes better than that of STLM (Fig. 5B), when  $\theta \geq 0.7$ . Finally, we further tested the performance of LTLM trained with examples of fashion-MNIST and found equivalent results (Fig. 5C and D). These results indicate that the offline training of LTLM does not strictly require external memories.

## Discussion

The mainstream research on machine learning has focused on the state of the art learning algorithms for networks to perform specified tasks, but even with the exploding success of DNNs, their learning ability is limited compared to that of the brain. It seems natural, at this point, to consider extending and modifying ANNs/DNNs to make them more similar to the brain. Building a system with continuous learning ability can lead us to the right direction. CLS theory proposes that memory systems relying on sparse representation may underlie our continuous learning (Norman and O'Reilly, 2003; O'Reilly et al., 2014). Inspired by this proposal, we constructed DynMat and tested it using three datasets. While we employed a simple learning scenario, the experimental results are promising. In DynMat, synapse-based memories allow fast computation of similarities between old and new examples, which make STLM's online learning possible. Furthermore, the estimated classification errors of STLM during the online learning of the third-object suggest that DynMat does not suffer catastrophic interference. Based on these observations, we propose that synapse-based memory and dynamic matching between examples, demonstrated in our study, could serve as components for continuous learning machine.

## Links to earlier models of continuous learning system

When a network is trained to perform a new task, its synaptic weights (as well as biases) are optimized despite the importance of old tasks, which leads to catastrophic interference. A line of studies proposed potential ways to alleviate catastrophic interference; see (Parisi et al., 2018). According to Parisi et al (Parisi et al., 2018), the earlier proposals rely on either weight-update regularization or network extensions. Specifically, the weights needed for earlier learning can be protected during new learning via regularizing weight updates (Kirkpatrick et al., 2017), or new weights or neurons can be added to incorporate new learning without interfering with old learning (Parisi et al., 2017). More recently, multiple studies proposed learning algorithms which do not require a large number of labeled examples (Koch et al., 2015; Santoro et al., 2016; Vinyals et al., 2016). They are often referred to as one-shot or a few-shot learning, in that networks can be trained with one (or a few) example(s) for task-learning. The aim of one-shot learning is to mimic the brain's ability to learn new objects instantly. For instance, humans can learn new species by looking at them just a few times (or even once).

We note that DynMat bears some similarity to these earlier proposals. First, matching between two examples has been proposed to be an essential computation for one-shot (or a few-shot) learning (Koch et al., 2015; Vinyals et al., 2016). DynMat indeed relies on the matching layer for its ability to learn without offline training. In DynMat, the matching between examples are performed naturally with synapses that store examples. Second, DynMat adds a new set of synaptic weights in ML to store novel examples, which is consistent with algorithms that expand networks to avoid catastrophic interference (Parisi et al., 2017, 2018). Third, the structure of DynMat is similar to those of neural networks with dual memory systems (Hattori, 2009; Lee et al., 2016), which are also inspired by CLS theory. However, unlike these networks with dual memory, short-term learning module of DynMat does not need to be trained, which makes online learning possible without interruption.

### Future direction of development of DynMat

DynMat presents a simple structure that can learn without catastrophic interference or offline training by utilizing synapse-based memory. It should be noted that DynMat has been tested in a limited scenario with simple tasks, but we plan to extend it to perform more complex functions in the future. Specifically, we will seek potential algorithms for DynMat to mimic functions of prefrontal cortex (PFC), which is known to perform executive functions such as decision-making (Miller and Cohen, 2001). To this end, DynMat will be extended in two ways.

First, we will develop unsupervised and reinforcement learning algorithms for DynMat (Hertz et al., 1991), as PFC is known to be associated with reward-based learning (Duverne and Koechlin, 2017; Miller and Cohen, 2001). The current DynMat requires labeled examples. Then, is it possible for DynMat to learn a new task without labeled examples? In principle, DynMat can be modified to learn without labeled examples, if two changes are introduced. First, with labeled examples, ML neurons are inserted when the present example is substantially different from the stored examples of the same class. However, if they are not available, comparison within a class would not be possible. That is, the comparison should be agnostic to classes. Second, LTLM needs to be a network that is trained with rewards, as suggested by reinforcement learning (Hertz et al., 1991). Since there is no fundamental restriction on LTLM structure, adopting one of the reinforcement learning algorithms to LTLM is possible.

Second, we will develop algorithms to regulate reciprocal interactions between feature detectors and DynMat, as PFC is reciprocally connected with sensory and motor areas (Bedwell et al., 2014). In this study, the feature detectors (ConvNets in ResNet) are not modified, and they provide afferent inputs to DynMat, but it does not receive afferent inputs from DynMat. This is consistent with the notion that high-order cognitive areas such as PFC) perform executive functions based on features extracted by low-order sensory cortices. However, it is increasingly clear that reciprocal interactions between low-order sensory and high-order cognitive areas are critical in cognitive functions of the brain; see (Bastos et al., 2015; Buschman and Miller, 2007; Fries et al., 2001) for instance. Therefore, we will investigate algorithms to establish reciprocal interactions between feature detectors and DynMat to improve DynMat's learning ability.

## Methods

DynMat was implemented by Pytorch (Paszke et al., 2017), a publicly available machine learning tool box.

### Structure of DynMat

DynMat consists of three different areas, matching layer (ML), short-term learning module (STLM) and long-term learning module (LTLM). Each neuron (i.e., a computing node) in ML is fully connected to the input layer (Fig. 1A) via one of the training example normalized to have a unit length (Eq. 1).

$$h_{i,k}^{ML} = \sum_j w_{ij}^{ML} \frac{x_j^k}{\|\vec{x}_k\|}, \text{ where } w_{ij}^{ML} = \frac{x_j^i}{\|\vec{x}_i\|} \quad (1)$$

, where  $h_{i,k}^{ML}$  represents the input to ML neuron  $m_i$  induced by  $k^{th}$  example; where  $x_j^k$  is the  $j^{th}$  component of  $k^{th}$  example; where  $w_{ij}^{ML}$  represents the connection from input node  $Ii$  to ML neuron  $m_i$ ; where  $x_j^k$  is the component of  $j^{th}$  component of  $k^{th}$  image, and  $\|\vec{x}_k\|$  represents the norm of  $k^{th}$  of image. All inputs to DynMat are also normalized to have a unit length (Eq. 1), and thus a synaptic input  $h_i$  to a ML neuron  $m_i$  is the cosine similarities between a current example and the stored ones. Whenever an example was introduced to the ML, we identified ML neurons that store examples belonging to the class of the present example. If any synaptic input  $h_i$  to these ML neurons is not greater than the pre-defined threshold value  $\theta$ , a new ML was added to ML. In brief, ML stores novel examples and calculates the similarities between the present and stored examples.

STLM is a linear layer, and each ML neuron projects one of STLM neurons (out of 3 in this study) according to Eq. 2.

$$h_{i,k}^{STLM} = \sum_j w_{ij}^{STLM} g(h_{j,k}^{ML}), \text{ where } w_{ij}^{STLM} = \begin{cases} 0, & i \neq c \\ 1, & i = c \end{cases}, g(x) = e^{-\frac{(x-1)^2}{0.5}} \quad (2)$$

, where  $h_{i,k}^{STLM}$  is the input to STLM neuron  $s_i$  elicited by  $k^{th}$  example; where  $w_{ij}^{STLM}$  represents the connection from ML neuron  $m_j$  to STLM neuron  $s_i$ ; where  $c$  represents the id of class, which runs from 0 to 2.  $g(x)$  is the activation of ML neuron used for STLM. That is, in DynMat, STLM memorizes the class of examples stored in the ML. When a stored example in ML is presented, it produces the maximal input ( $h_i=1$ ) to the ML neuron  $m_i$ , which was added when the example was presented. Consequently, a STLM neuron connected to this ML neuron, which is determined by the class of example (Eq. 2), will produce the strongest output. With the ‘winner-take-all’ rule applied, STLM retrieves the class of the present example. However, this operation can be corrupted with stochastic activations of other ML neurons. To suppress this stochastic corruption, non-linear summation of ML outputs is used to calculate STLM neuron activation functions (Eq. 2).

LTLM is a multilayer perceptron (MLP) with a single hidden layer (Fig. 1A). LTLM is also connected to ML (Eq. 3) and thus trained to classify ML outputs.

$$h_{i,k}^{LTLM} = \sum_j w_{ij}^{LTLM} h_{j,k}^{ML} \quad (3)$$

, where  $h_{i,k}^{STLM}$  is the input to LTLM neuron  $l_i$  elicited by  $k^{th}$  example; where  $h_{j,k}^{STLM}$  is the input to STLM neuron  $s_j$  elicited by  $k^{th}$  example; where  $w_{ij}^{LTLM}$  represents the connection from ML neuron  $m_j$  to LTLM neuron  $l_i$ .

We used backpropagation to train LTLM. The error was measured by Mean-Squared estimates, which is implemented with `MSELoss` in Pytorch (Paszke et al., 2017). During its learning, we used two learning phases. The first phase lasted 4000 (8000 for training with CIFAR-100 dataset) epochs with learning rate  $\lambda=1e^{-4}$ , and the second phase lasted 2000 epochs (4000 for CIFAR-100 dataset) with learning rate  $\lambda=1e^{-5}$ . For all training of LTLM except one exception, we used 100 examples in a single patch: When we trained LTLM with examples stored in DynMat, 10 examples, instead of 100 ones, constituted a single batch.

## Database

To evaluate the learning ability of DynMat, we used three datasets, MNIST (LeCun et al., 1998), fashion-MNIST (Xiao et al., 2017) and CIFAR-100 (Krizhevsky, 2009). MNIST includes 60,000 training and 10,000 test images of handwritten digits (0-9). Each image consists of 28-by-28 8-bit grey pixels. MNIST has been used in numerous studies, but it is now considered an easy benchmark. The fashion-MNIST dataset was proposed as a drop-in replacement of MNIST. It directly corresponds to MNIST in terms of the number of class, input size and the sizes of test and training set. It, however, includes examples of 10 fashion items such as t-shirts and shoes, instead of handwritten digits. CIFAR-100 is the collection of 100 classes of items ranging from animals to man-made devices. Each class has 500 training and 100 test examples, each of which is a 32-by-32 color image. All examples of the MNIST and fashion-MNIST are normalized to have unit length by dividing its norm (Eq.1) before introducing to ML.

## Feature detectors for DynMat when it is used an embedded learning system

Since He et al. (He et al., 2015, 2016) proposed the residual deep neural network (ResNet) to address vanishing gradient in DNNs, it has been widely adopted, and its variants such as DenseNet (Huang et al., 2017) and ResNeXt (Xie et al., 2017) have been proposed. Due to its simplicity and demonstrated learning ability, we selected ResNet to extract features to train DynMat as an embedded learning system. Specifically, the pre-trained ResNet is used in our study (Idelbayev, 2018). It is important to note that this ResNet is trained with CIFAR-10 dataset rather than CIFAR-100, which is used to test the learning capability of ResNet.

## Acknowledgement

JHL wishes to thank the Allen Institute founders, Paul G. Allen and Jody Allen, for their vision, encouragement and support.

## References

Bastos, A.M., Vezoli, J., Bosman, C.A., Schoffelen, J.-M., Oostenveld, R., Dowdall, J.R., De Weerd, P., Kennedy, H., and Fries, P. (2015). Visual Areas Exert Feedforward and Feedback Influences through Distinct Frequency Channels. *Neuron* 390–401.

Bedwell, S.A., Billett, E.E., Crofts, J.J., and Tinsley, C.J. (2014). The topology of connections between rat prefrontal, motor and sensory cortices. *Front. Syst. Neurosci.* 8, 1–10.

Buschman, T.J., and Miller, E.K. (2007). Top-down versus bottom-up control of attention in the prefrontal and posterior parietal cortices. *Science* 315, 1860–1862.

Choi, J., Sim, S., Kim, J., Choi, D. Il, Oh, J., Ye, S., Lee, J., Kim, T., Ko, H., and Lim, C. (2018). Interregional synaptic maps among engram cells underlie memory formation. *435*, 430–435.

Diehl, P., and Cook, M. (2015). Unsupervised learning of digit recognition using spike-timing-dependent plasticity. *Front. Comput. Neurosci.* 9, 99.

Duverne, S., and Koechlin, E. (2017). Rewards and Cognitive Control in the Human Prefrontal Cortex. *Cereb. Cortex* 27, 5024–5039.

Fries, P., Reynolds, J.H., Rorie, A.E., and Desimone, R. (2001). Modulation of oscillatory neuronal synchronization by selective visual attention. *Science* 291, 1560–1563.

Graves, A., Wayne, G., and Danihelka, I. (2014). Neural Turing Machines. *CoRR abs/1410.5*, 1410.5401.

Hattori, M. (2009). Avoiding catastrophic forgetting by a dual-network memory model using a chaotic neural network. *Int. J. Electr. Comput. Eng.* 3, 853–857.

He, K., Zhang, X., Ren, S., and Sun, J. (2015). Deep residual learning for image Recognition. *CoRR abs/1512.0*, 1512.03385.

He, K., Zhang, X., Ren, S., and Sun, J. (2016). Identity mappings in deep residual networks. *CoRR abs/1603.0*, 1603.05027.

Hertz, J., Krogh, A., and Palmer, R. (1991). Introduciton to the theory of neural computation (Westview).

Hochreiter, S., and Urgen Schmidhuber, J. (1997). Long Short-Term Memory. *Neural Comput.* 9, 1735–1780.

Huang, G., Liu, Z., Van Der Maaten, L., and Weinberger, K.Q. (2017). Densely connected convolutional networks. Proc. - 30th IEEE Conf. Comput. Vis. Pattern Recognition, CVPR 2017 2017–Janua, 2261–2269.

Idelbayev, Y. (2018). *pytorch\_resnet\_cifar10*. Github-Repository [https://github.com/akamaster/pytorch\\_resnet\\_cifar1](https://github.com/akamaster/pytorch_resnet_cifar1).

Kirkpatrick, J., Pascanu, R., Rabinowitz, N., Veness, J., Desjardins, G., Rusu, A.A., Milan, K., Quan, J., Ramalho, T., Grabska-Barwinska, A., et al. (2017). Overcoming catastrophic forgetting in neural networks. *114*, 3521–3526.

Kleim, J. a, Freeman, J.H., Bruneau, R., Nolan, B.C., Cooper, N.R., Zook, A., and Walters, D. (2002). Synapse formation is associated with memory storage in the cerebellum. *Proc Natl Acad Sci U S A* *99*, 13228–13231.

Koch, G., Zemel, R., and Salakhutdinov, R. (2015). Siamese Neural Networks for One-Shot Image Recognition. In *ICML*, p.

Krizhevsky, A. (2009). Learning Multiple Layers of Features from Tiny Images. Tech. Report, Univ. Toronto 1–60.

Lecun, Y., Bengio, Y., and Hinton, G. (2015). Deep learning. *Nature* *521*, 436–444.

LeCun, Y., Bottou, L., Bengio, Y., and Haffner, P. (1998). Gradient-Based Learning Applied to Document Recognition. *PROC. IEEE*.

Lee, S.W., Lee, C.Y., Kwak, D.H., Kim, J., Kim, J., and Zhang, B.T. (2016). Dual-memory deep learning architectures for lifelong learning of everyday human behaviors. *Int. Jt. Conf. Artif. Intell. 2016–Janua*, 1669–1675.

Lüders, B., Schläger, M., Korach, A., and Risi, S. (2017). Continual and One-Shot Learning through Neural Networks with Dynamic External Memory. *Lect. Notes Comput. Sci.* *10199*.

Mayford, M., Siegelbaum, S.A., and Kandel, E.R. (2012). Synapses and Memory Storage. *Cold Spring Harb Perspect Biol.* *4*, a005751.

Miller, E.K., and Cohen, J.D. (2001). An Integrative Theory of Prefrontal Cortex Function. 167–202.

Mongillo, G., Barak, O., and Tsodyks, M. (2008). Synaptic theory of working memory. *Science* *319*, 1543–1546.

Norman, K. a, and O'Reilly, R.C. (2003). Modeling hippocampal and neocortical contributions to recognition memory: a complementary-learning-systems approach. *Psychol. Rev.* *110*, 611–646.

O'Reilly, R.C., Bhattacharyya, R., Howard, M.D., and Ketz, N. (2014). Complementary learning systems. *Cogn. Sci.* *38*, 1229–1248.

Parisi, G.I., Tani, J., Weber, C., and Wermter, S. (2017). Lifelong learning of human actions with deep neural network self-organization. *Neural Networks* *96*, 137–149.

Parisi, G.I., Kemker, R., Part, J.L., Kanan, C., and Wermter, S. (2018). Continual Lifelong Learning with Neural Networks: A Review. *CoRR abs/1802.0*, 1802.07569.

Paszke, A., Gross, S., Chintala, S., Chanan, Gregory Yang, E., DeVito, Z., Lin, Zeming Desmaison, A., Antiga, L., and Lerer, A. (2017). Automatic differentiation in PyTorch. In *NIPS-W*, p.

Ratcliff, R. (1990). Connectionist Models of Recognition Memory: Constraints Imposed by Learning and Forgetting Functions. *Psychol. Rev.* *97*, 285–308.

Santoro, A., Bartunov, S., Botvinick, M., Wierstra, D., and Lillicrap, T. (2016). One-shot Learning with Memory-Augmented Neural Networks. *CoRR abs/1605.0*, 1605.06065.

Schmidhuber, J. (2015). Deep Learning in neural networks: An overview. *Neural Networks* *61*, 85–117.

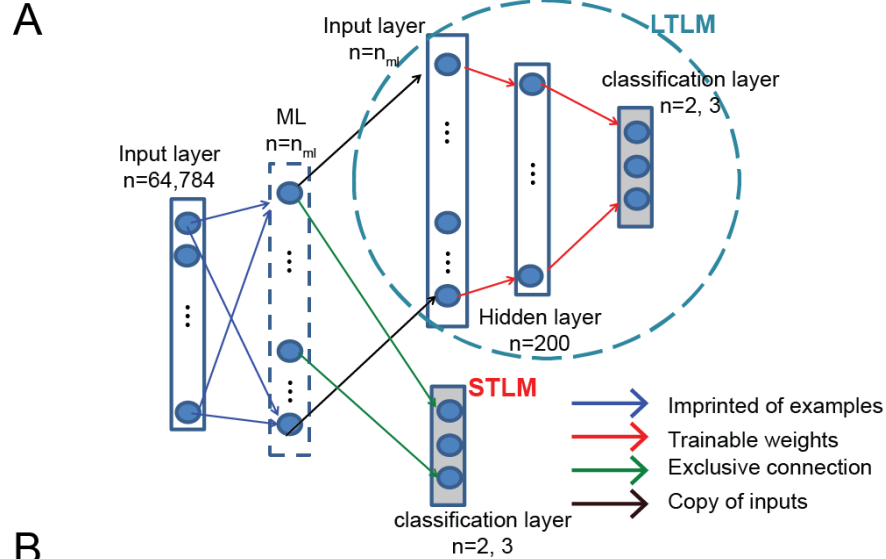
Vargas, R., Mosavi, A., and Ruiz, L. (2017). Deep Learning : a Review Deep Learning : a Review. *Adv. Intell. Syst. Comput.* *5*.

Vinyals, O., Blundell, C., Lillicrap, T., Kavukcuoglu, K., and Wierstra, D. (2016). Matching Networks for One Shot Learning. p.

Xiao, H., Rasul, K., and Vollgraf, R. (2017). Fashion-MNIST: a Novel Image Dataset for Benchmarking Machine Learning Algorithms. *CoRR abs/1708.0*, 1708.07747.

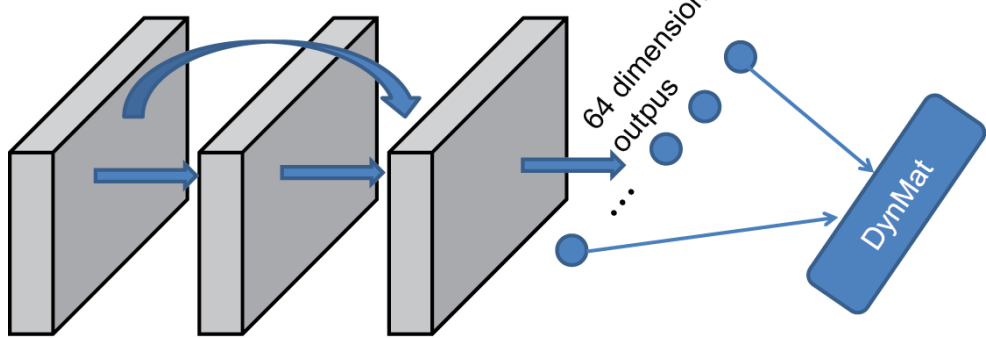
Xie, S., Girshick, R., Dollár, P., Tu, Z., and He, K. (2017). Aggregated residual transformations for deep neural networks. *Proc. - 30th IEEE Conf. Comput. Vis. Pattern Recognition, CVPR 2017 2017-Janua*, 5987–5995.

## Figures



**B**

ConvNets in the ResNet



**C**

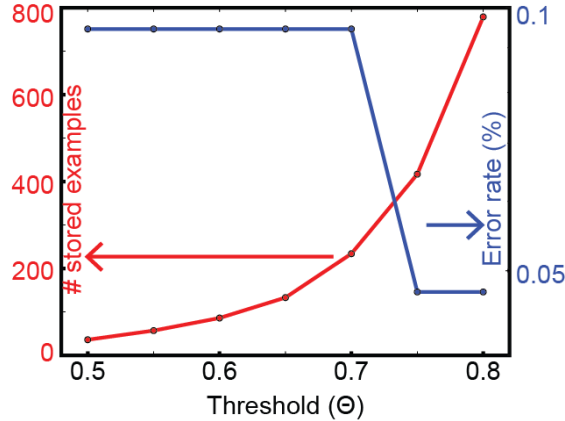
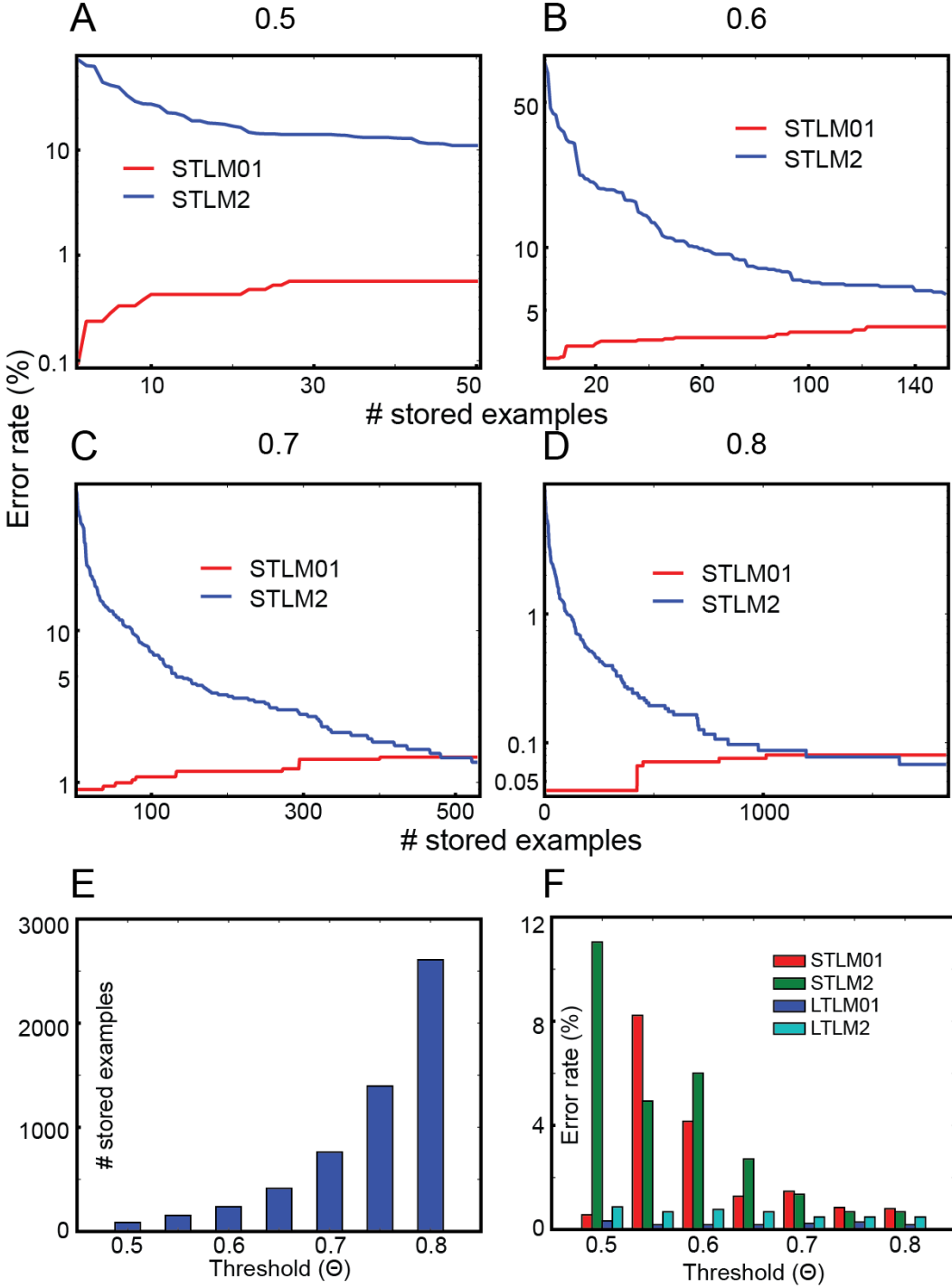
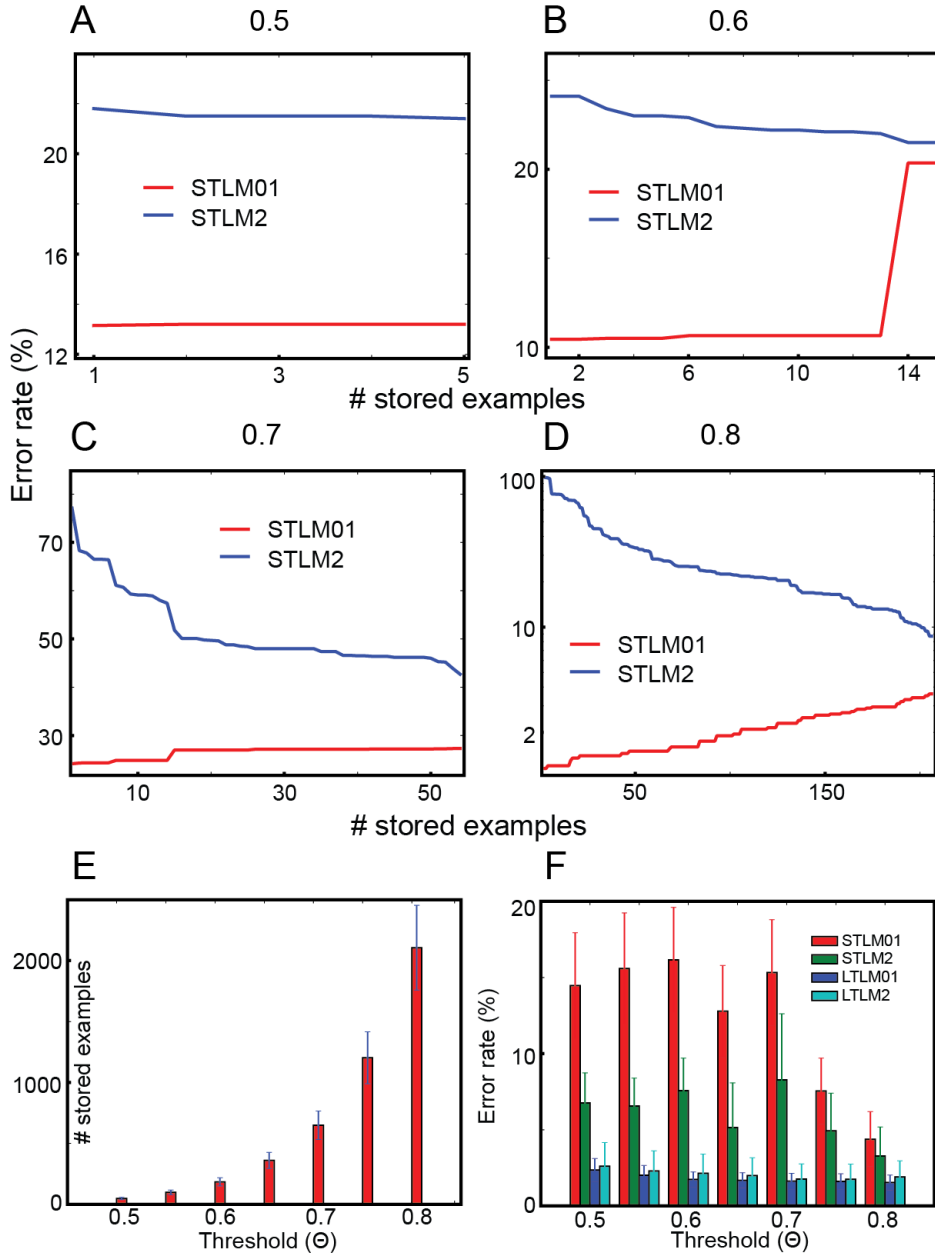


Figure 1: Structure of DynMat and basic mechanism. (A), The schematics of DynMat consisting of matching layer (ML), short-term learning module (STLM) and long-term learning module (LTLM). In principle, DynMat is a collection of layered neurons (i.e., the computing nodes). The size of each layer is shown in the figure, and the input size is 784 for MNIST and fashion-MNIST and 64 for CIFAR-100 datasets. The arrows represent synaptic weights, and their properties are summarized in color codes. See Methods for details. (B), The schematics of DynMat embedded to ResNet. The ResNet adopted from the public repository (Idelbayev, 2018) generates 64 dimensional outputs, which are fed to the linear classifier. In this study, the linear classifier is replaced with DynMat (C), The dependency of ML size and the error rate of LTLM on the threshold ( $\Theta$ ). Specifically, the size and error rate are measured using examples of two digits (0 and 1).



**Figure 2: DynMat's learning with MNIST dataset.** (A)-(D), The error rate of STLM, during the exposure of the examples of new digit 2, on the first two testing examples (digits 0 and 1) and the third example (digit 2). STLM01 represents the error rate on 0 and 1, whereas STLM2 represents the error rate on 2. These error rates depend on the threshold ( $\theta$ ), and thus we measured them by varying the threshold from 0.5 to 0.8. The results with  $\theta=0.5, 0.6, 0.7$  and 0.8 are shown in (A), (B), (C) and (D), respectively. The x-axis represents the number of examples of digit 2 stored in ML. (E), The total number of examples stored in ML depending on the threshold value ( $\theta$ ). (F), The error rate of STLM and LTLM. LTLM01 (STLM01) represents the error rate of LTLM (STLM) on digits 0 and 1, and LTLM2 (STLM2) represents the error rate of LTLM (STLM) on digit 2.



**Figure 3: DynMat’s learning with fashion-MNIST dataset.** (A)-(D), The error rate of STLM, during the exposure of examples of the third item, on the testing examples of the first two fashion items and the third fashion item; they are selected randomly out of 10 items in the dataset. STLM01 represents the error rate on the first two items, whereas STLM2 represents the error rate on the third item. These error rates depend on the threshold ( $\Theta$ ), and thus we measured them by varying the threshold from 0.5 to 0.8. The results with  $\Theta=0.5, 0.6, 0.7$  and 0.8 are shown in (A), (B), (C) and (D), respectively. The  $x$ -axis represents the number of examples of third-fashion item stored in ML. (E), The total number of examples stored in ML depending on the threshold value ( $\Theta$ ). We illustrated the mean values and standard errors calculated from 10 independent experiments, in which 3 fashion items are independently chosen; the results suggest that the variance is high. (F), The error rate of STLM and LTLM. LTLM01 (STLM01) represents the error rate of LTLM (STLM) on the first two items, and LTLM2 (STLM2) represents the error rate of LTLM (STLM) on the third item. We illustrated the mean values and standard errors calculated from 10 independent experiments.

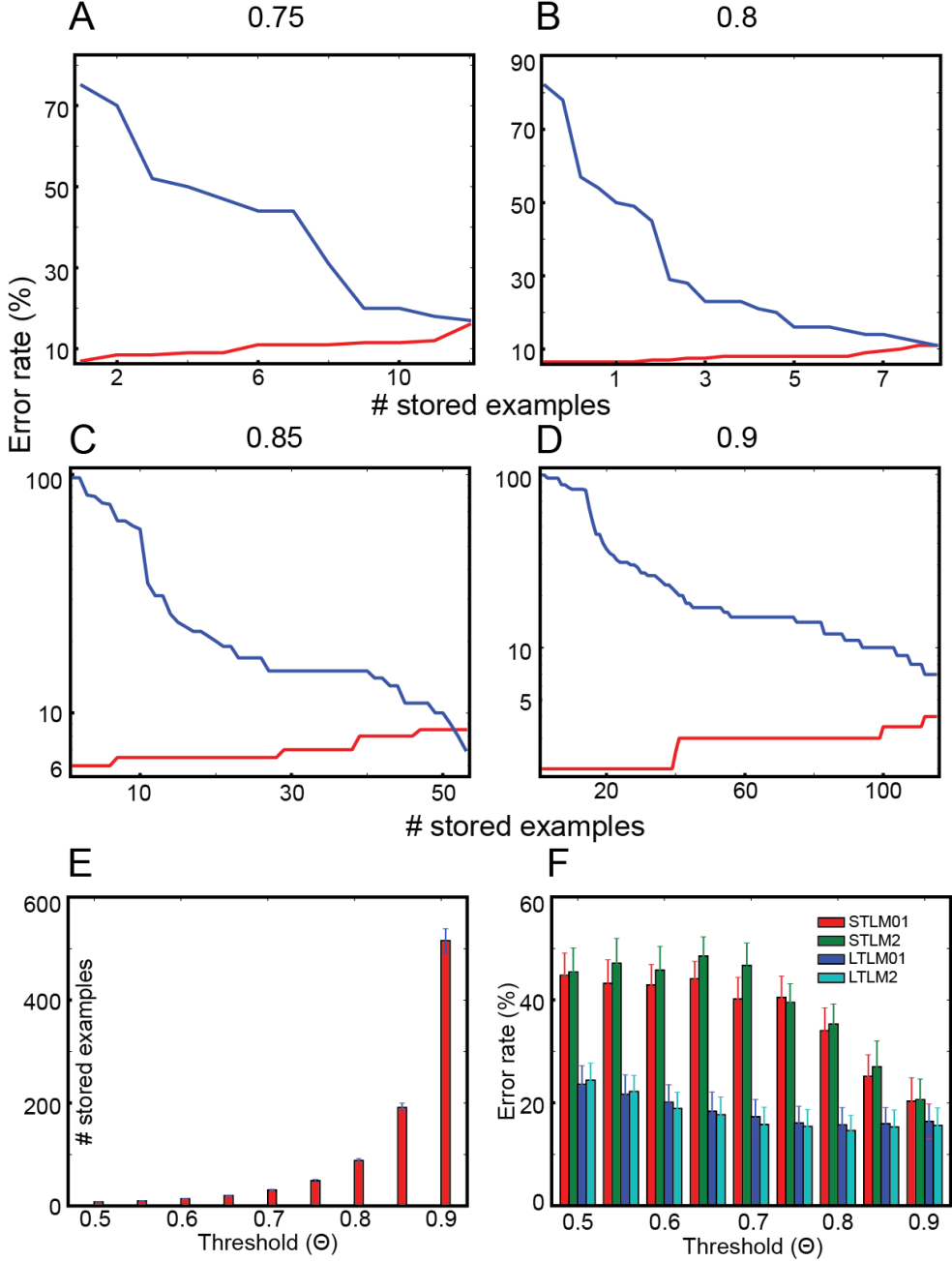


**Figure 4: DynMat's learning as an embedded learning system.** (A)-(D), The error rate of STLM, during the exposure of examples of the third item, on the testing examples of the first two visual items and the third-visual object item; they are selected randomly out of 100 visual objects in CIFAR-100 dataset. STLM01 represents the error rate on the first two visual objects, whereas STLM2 represents the error rate on the third visual object. These error rates depend on the threshold ( $\theta$ ), and thus we measured them by varying the threshold from 0.75 to 0.9. The results with  $\theta=0.75, 0.8, 0.85$  and  $0.9$  are shown in (A), (B), (C) and (D), respectively. The x-axis represents the number of examples of third-visual object stored in ML. (E), The total number of examples stored in ML depending on the threshold value ( $\theta$ ). We illustrated the mean values and standard errors calculated from 10 independent experiments, in which 3 visual objects are independently chosen; the results suggest that the variance is high. (F), The error rate of STLM and LTLM. LTLM01 (STLM01) represents the error rate of LTLM (STLM) on the first two items, and LTLM2 (STLM2) represents the error rate of LTLM (STLM) on the third item. We illustrated the mean values and standard errors calculated from 10 independent experiments.

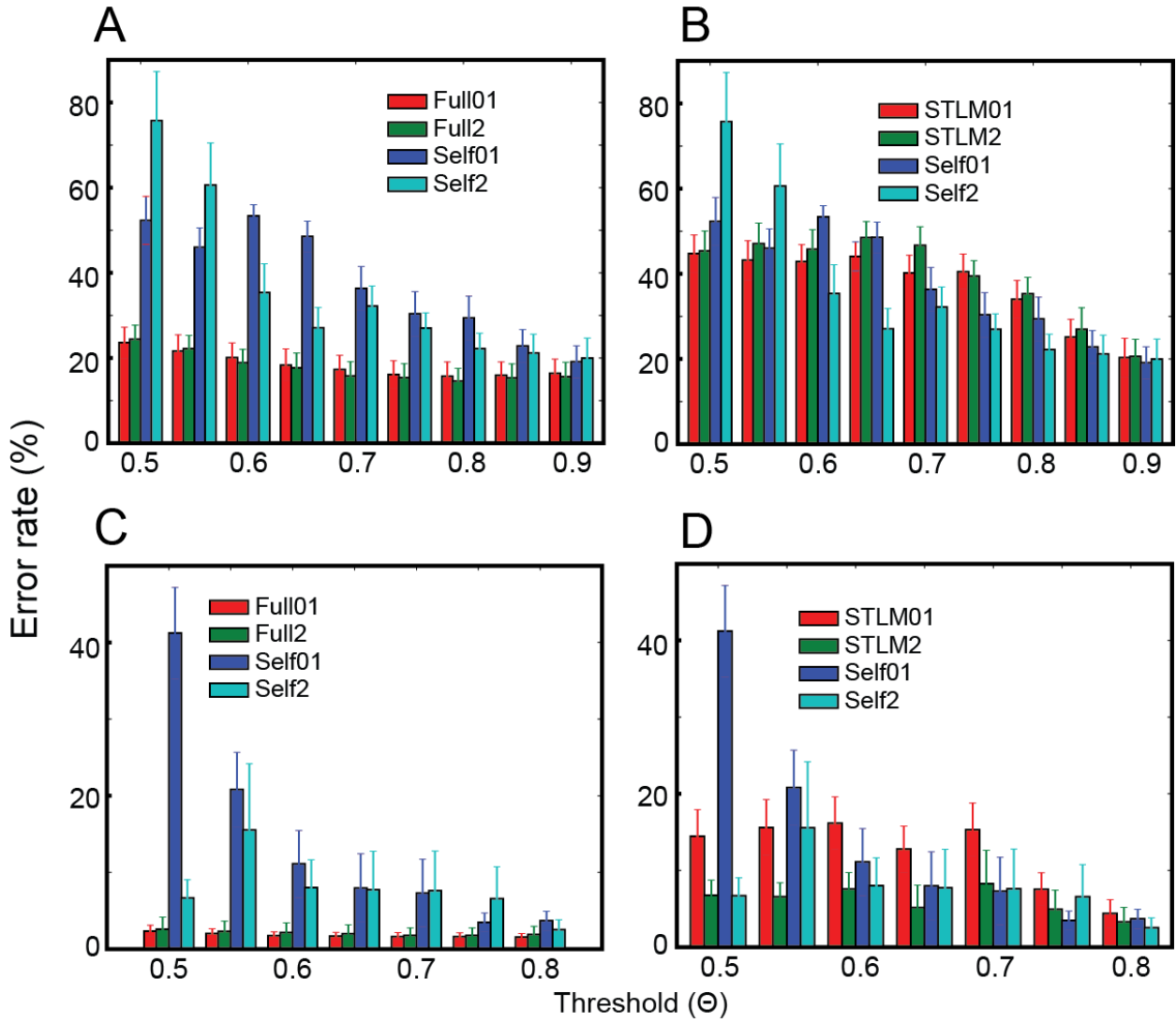


**Figure 5: The classification fidelity of LTLM. LTLM can be trained with the examples stored in ML.** We compare the classification fidelity of LTLM trained with the examples stored in ML to that of LTLM trained with the full training set, depending on the threshold ( $\theta$ ). **(B)**, The error rates (shown in blue and cyan) of LTLM trained with examples of CIFAR-100 stored in ML and the error rates (shown in red and green) of LTLM trained with the full training set. Full01 and Full2 represent the error rate of LTLM, trained with the full training set, on the first two classes and the third class, respectively. In contrast, Self01 and Self2 represent the error rate of LTLM, trained with examples stored in ML, on the first two classes and the third class, respectively. **(B)**, The comparison between error rates of LTML trained with the examples stored in ML and the error rates of STLM (depending on the threshold  $\theta$ ). STLM01 and STLM2 represent the error rate of STLM on the first two classes and the third class, respectively. **(C)** and **(D)**, the same as (A) and (B) but DynMat is trained with fashion-MNIST, instead of CIFAR-100. We trained LTLM using raw outputs of ResNets (with the fully connected layer removed), their normalized outputs and outputs of ML.